AIMS Materials Science, 7(5): 632–649.
DOI: 10.3934/matersci.2020.5.632
Received: 02 June 2020
Accepted: 23 September 2020
Published: 28 September 2020

http://www.aimspress.com/journal/Materials

Research article

Ion aggregation in complexes of alkali metal iodides and poly(ethylene oxide) or pentaglyme studied by molecular dynamics

Andrzej Eilmes*

Jagiellonian University, Faculty of Chemistry, Gronostajowa 2, 30-387 Kraków, Poland

* **Correspondence:** Email: eilmes@chemia.uj.edu.pl; Tel: +48126862377; Fax: +48126862750.

Supplementary

Table S1. Me-I distances d (in Å) and binding energies E_b (in kcal/mol) obtained from quantum chemical (QC) MP2/def2-TZVP calculations and molecular mechanics using FF0 of FF1 force field. ΔE_b are the differences E_b(FF) − E_b(QC).

Me	QC		FF0			FF1		
	d	E_b	d	E_b	ΔE_b	d	E_b	ΔE_b
Li	2.40	−135.6	2.17	−179.0	−43.5	2.42	−145.6	−10.0
Na	2.72	−119.4	2.67	−133.1	−13.7	2.72	−126.0	−6.5
K	3.08	−104.2	3.03	−114.2	−10.0	3.08	−109.5	−5.3
Rb	3.24	−98.3	3.26	−105.2	−6.9	3.26	−103.4	−5.1
Cs	3.38	−95.0	3.38	−102.2	−7.2	3.41	−99.3	−4.3

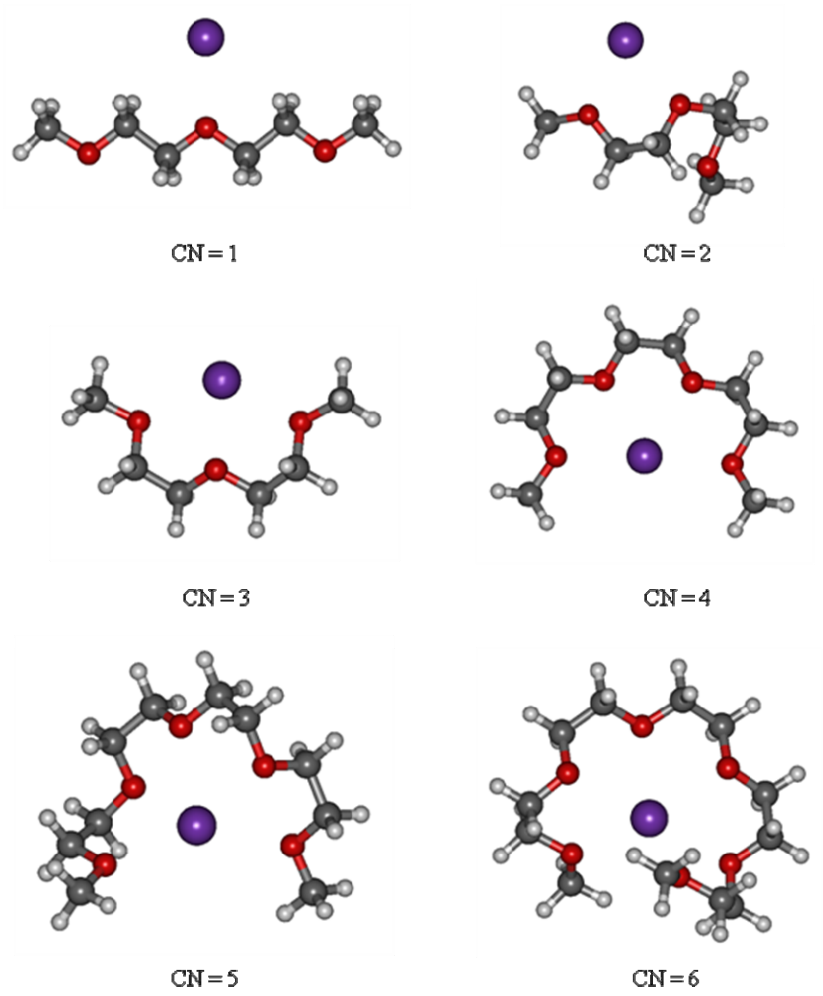

Figure S1. Structues of K^+ complexes with oligoglymes optimized in MP2/def2-TZVP calculations for different values of the coordination number CN.

Table S2. Me-O distances (in Å) in Me^{+}-oligoglyme complexes obtained for different coordination numbers (CNs) from quantum chemical calculations and molecular mechanics with FF0 of FF1 force field.

	CN	Li	Na	K	Rb	Cs
QC	1	1.82	2.20	2.60	2.78	2.96
	2	1.86,1.87	2.23, 2.24	2.62, 2.63	2.78, 2.80	2.94, 2.96
	3	1.92,1.92,1.93	2.27, 2 × 2.30	2.67, 2 × 2.69	3 × 2.84	2 × 3.00, 3.02
	4	2 × 1.98, 2 × 2.00	2 × 2.32, 2 × 2.33	2 × 2.70, 2 × 2.72	2 × 2.87, 2 × 2.88	4 × 3.05
	5	2 × 1.97, 2.01, 2.07, 2.08	2.32, 2.33, 2 × 2.37, 2.38	2 × 2.72,2 × 2.74, 2.75	2 × 2.88, 2 × 2.89, 2.92	3.05, 3.06, 3.07, 3.09, 3.12
	6	2 × 2.06, 2 × 2.20, 2 × 2.27	2 × 2.33, 2 × 2.37, 2 ×2.39	2 × 2.74, 2 × 2.75, 2 × 2.77	2 × 2.89, 2 × 2.92, 2 × 2.93	2 × 3.07, 2 × 3.11, 2 × 3.13
FF0	1	1.95	2.40	2.76	2.99	3.11
	2	2 × 2.00	2 × 2.45	2 × 2.80	3.01, 3.02	2 × 3.13
	3	2 × 2.03,2.04	2.47, 2 × 2.49	2.82, 2 × 2.84	3 × 3.05	2 × 3.16, 3.17
	4	2 × 2.07, 2 × 2.08	2 × 2.50, 2 × 2.51	2 × 2.85, 2 × 2.86	2 × 3.06, 2 × 3.07	3 × 3.18
	5	2.07, 2.08, 2.10, 2 × 2.13	2.50, 2.51, 2 × 2.52, 2.54	2.85, 3 × 2.87, 2.88	2 × 3.07, 3 × 3.09	2 × 3.19, 2 × 3.20, 3.21
	6	2 × 2.15, 2 × 2.21, 2 × 2.24	2 × 2.52, 2 × 2.53, 2 × 2.55	4 × 2.88, 2 × 2.90	2 × 3.08, 2 × 3.10, 2 × 3.11	2 × 3.19, 2 × 3.22, 2 × 3.23
FF1	1	1.87	2.22	2.63	2.78	2.99
	2	2 × 1.92	2 × 2.27	2.66, 2.67	2.81, 2.82	3.00, 3.01
	3	2 × 1.95,1.97	3 × 2.30	2.69, 2 × 2.71	3 × 2.85	2 × 3.04, 3.05
	4	2 × 2.00, 2 × 2.01	2 × 2.32, 2× 2.34	4 × 2.73	4 × 2.88	4 × 3.07
	5	2.01, 2.02, 2.05, 2 × 2.09	2.32, 2.33, 2 × 2.36, 2.37	2.72, 2 × 2.74, 2.75, 2.76	2.88, 2.89, 2 × 2.90, 2.91	2 × 3.08, 2 × 3.09, 3.10
	6	2 × 2.04, 2 × 2.13, 2 × 2.37	2 × 2.36, 4 × 2.41	2 × 2.74, 2 × 2.76, 2 × 2.77	4 × 2.90, 2 × 2.92	2 × 3.09, 2 × 3.10, 2 × 3.11

Table S3. Binding energies (in kcal/mol) of Me^+ to oligoglyme molecule obtained for different coordination numbers (CNs) from quantum chemical calculations and molecular mechanics with FF0 of FF1 force field. Values in parentheses are the differences E_b(FF) − E_b(QC).

	CN	Li	Na	K	Rb	Cs
QC	1	−37.8	−25.2	−17.2	−14.6	−13.0
	2	−68.1	−47.7	−35.0	−30.7	−28.1
	3	−86.3	−60.4	−44.4	−38.9	−35.4
	4	−104.6	−75.3	−55.8	−49.0	−44.5
	5	−117.7	−87.7	−66.2	−58.4	−53.4
	6	−126.0	−98.3	−76.2	−67.5	−61.5
FF0	1	−30.1 (7.7)	−17.7 (7.5)	−12.5 (4.7)	−10.5 (4.1)	−9.7 (3.3)
	2	−56.8 (11.4)	−37.4 (10.3)	−28.6 (6.4)	−24.8 (5.9)	−23.4 (4.7)
	3	−75.1 (11.2)	−49.5 (10.9)	−37.9 (6.5)	−33.0 (5.9)	−31.1 (4.3)
	4	−92.1 (12.4)	−63.0 (12.3)	−48.6 (7.2)	−42.5 (6.5)	−40.0 (4.5)
	5	−105.0 (12.7)	−75.0 (12.7)	−58.7 (7.5)	−51.7 (6.7)	−48.8 (4.5)
	6	−115.6 (10.4)	−85.6 (12.7)	−68.3 (7.9)	−60.4 (7.0)	−57.0 (4.5)
FF1	1	−33.5 (4.3)	−21.8 (3.4)	−14.2 (3.0)	−12.5 (2.1)	−10.6 (2.4)
	2	−61.3 (4.0)	−43.8 (4.0)	−31.4 (3.6)	−28.5 (2.2)	−25.2 (2.9)
	3	−78.5 (7.8)	−56.7 (3.7)	−41.2 (3.1)	−37.5 (1.4)	−33.2 (2.2)
	4	−94.0 (10.5)	−70.8 (4.4)	−52.4 (3.4)	−47.8 (1.2)	−42.5 (1.9)
	5	−105.6 (12.1)	−80.6 (7.1)	−61.8 (4.4)	−56.0 (2.4)	−50.5 (2.9)
	6	−107.8 (18.1)	−91.1 (7.2)	−68.5 (7.6)	−62.6 (4.9)	−55.6 (5.9)

Table S4. Modified pair interactions of the Lennard−Jones potential in the FF1 force field.

Pair	σ, Å	ε, kcal/mol
Li-I	3.2	0.2
Na-I	3.37	0.36
K-I	3.72	0.43
Rb-I	3.88	0.48
Li-O	2.435	0.12
Na-O	2.66	0.21
K-O	3.02	0.24
Rb-O	3.13	0.27
Cs-O	3.30	0.30

*Note: Vdwtype: LENNARD−JONES; radiustype: SIGMA; radiussize: DIAMETER.

Table S5. Densities (in g/cm^3) of simulated electrolytes averaged over last 5 ns of the MD trajectory.

	T, °C	Li	Na	K	Rb	Cs
$(PEO)_{30}MeI$	40	1.232 ± 0.008	1.237 ± 0.007	1.246 ± 0.007	1.283 ± 0.007	1.316 ± 0.008
	65	1.206 ± 0.008	1.215 ± 0.008	1.223 ± 0.008	1.254 ± 0.008	1.288 ± 0.008
	100	1.172 ± 0.009	1.178 ± 0.009	1.185 ± 0.009	1.218 ± 0.009	1.248 ± 0.009
	150	1.125 ± 0.009	1.131 ± 0.009	1.139 ± 0.009	1.171 ± 0.01	1.201 ± 0.01
	200	1.081 ± 0.01	1.088 ± 0.01	1.097 ± 0.01	1.127 ± 0.01	1.156 ± 0.01
Pentaglyme/MeI	40	1.128 ± 0.006	1.140 ± 0.006	1.143 ± 0.006	1.174 ± 0.006	1.205 ± 0.007
	65	1.100 ± 0.006	1.108 ± 0.006	1.114 ± 0.006	1.146 ± 0.007	1.174 ± 0.007
	100	1.064 ± 0.007	1.071 ± 0.007	1.078 ± 0.007	1.108 ± 0.007	1.136 ± 0.007
	150	1.011 ± 0.007	1.019 ± 0.007	1.025 ± 0.007	1.053 ± 0.007	1.082 ± 0.008
	200	0.957 ± 0.008	0.965 ± 0.008	0.971 ± 0.008	0.998 ± 0.008	1.025 ± 0.008

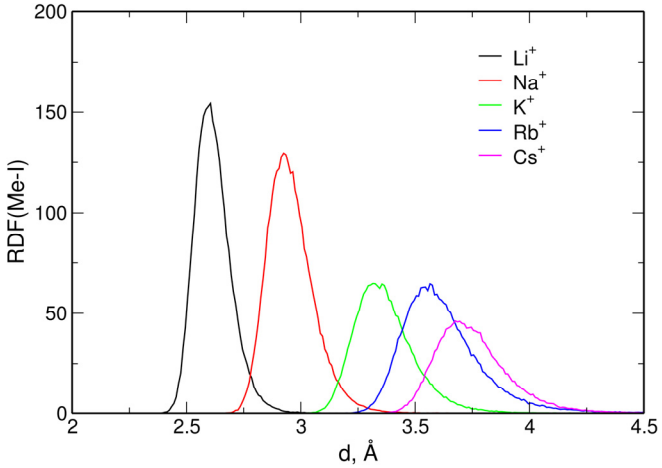

Figure S2. Radial distribution functions for Me-I pairs in $(PEO)_{30}MeI$ electrolytes obtained from MD simulations.

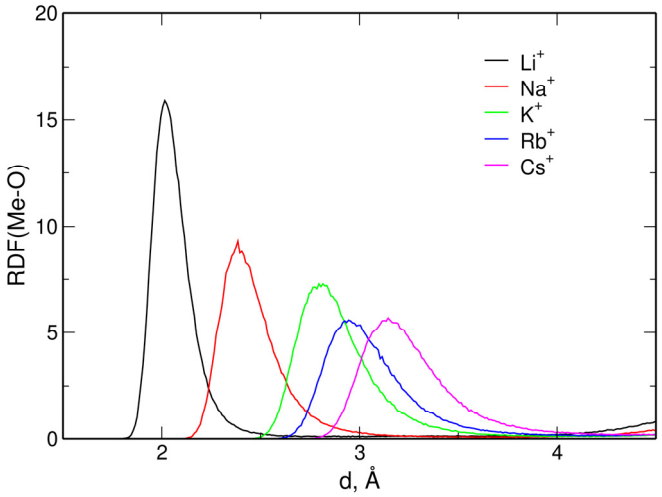

Figure S3. Radial distribution functions for Me-O atom pairs in $(PEO)_{30}MeI$ electrolytes obtained from MD simulations.

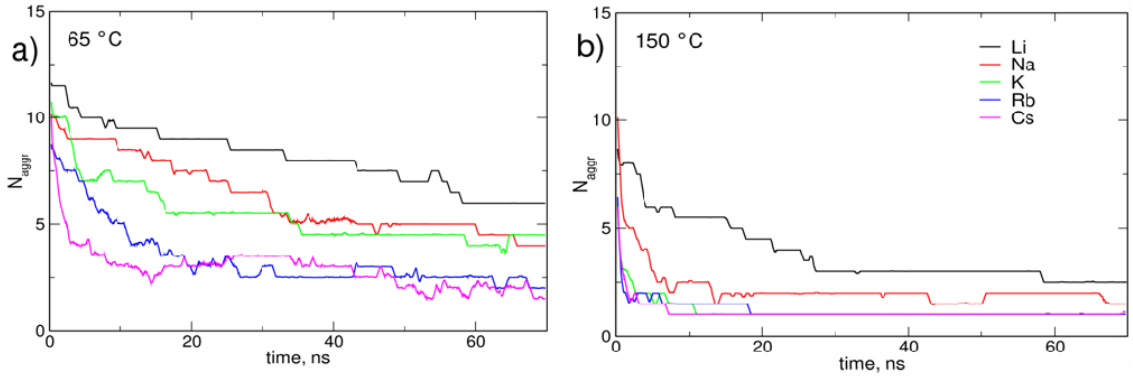

Figure S4. Changes in the number of ion aggregates N_{aggr} in the sample during MD simulations of $(PEO)_{30}$MeI electrolytes at (a) 65 ºC and (b) 150 ºC. Moving average has been used to smooth the plot.

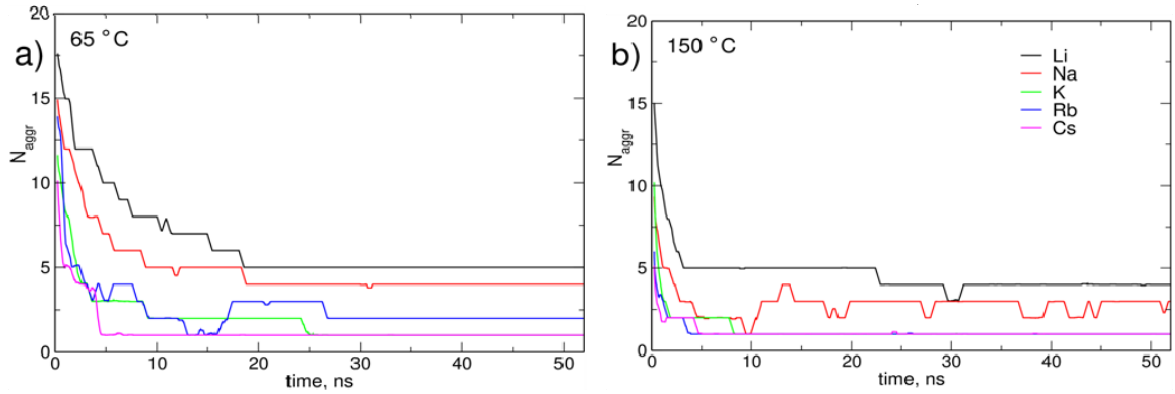

Figure S5. Changes in the number of ion aggregates N_{aggr} in the sample during MD simulations of pentaglyme/MeI electrolytes at (a) 65 ºC and (b) 150 ºC. Moving average has been used to smooth the plot.

Table S6. Average number of ion aggregates and its standard deviation during last 5 ns of MD simulations for pentaglyme/MeI electrolytes.

T, °C	Li	Na	K	Rb	Cs
40	7.00 ± 0.01	6.00 ± 0.01	2.82 ± 0.38	1.98 ± 0.15	1.00 ± 0.01
65	5.00 ± 0.01	4.00 ± 0.01	1.00 ± 0.01	2.00 ± 0.01	1.00 ± 0.01
100	5.00 ± 0.01	3.00 ± 0.04	1.00 ± 0.01	1.51 ± 0.50	1.00 ± 0.01
150	4.00 ± 0.08	2.93 ± 0.25	1.00 ± 0.03	1.00 ± 0.01	1.00 ± 0.01
200	4.00 ± 0.03	2.81 ± 0.50	1.00 ± 0.04	1.03 ± 0.16	1.00 ± 0.04

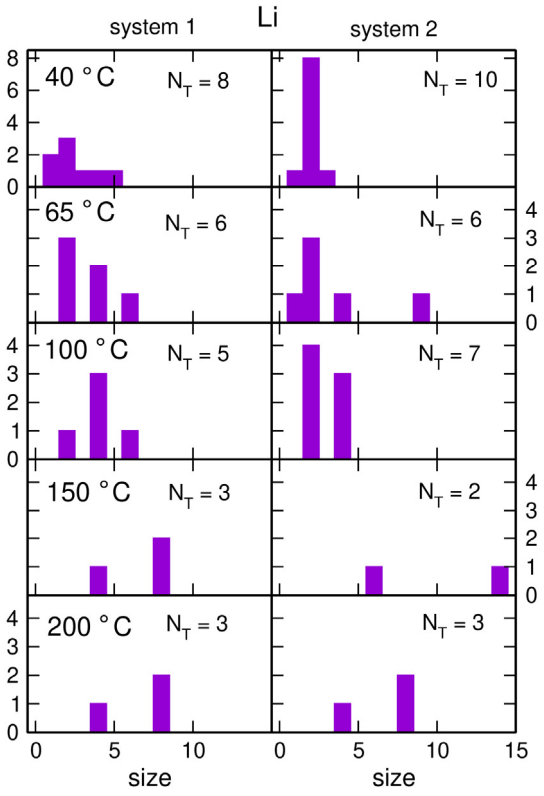

Figure S6. The number of different−sized aggregates in two series of $(PEO)_{30}LiI$ systems at the end of the MD trajectory. N_T is the total number of aggregates.

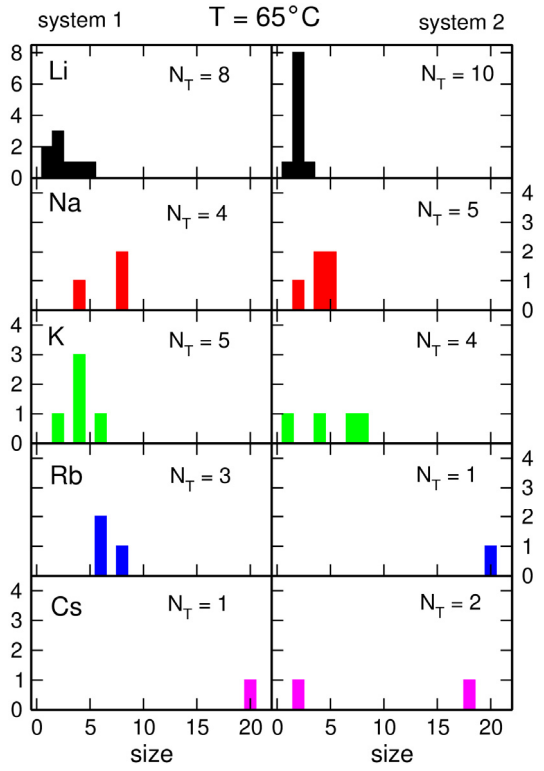

Figure S7. The number of different−sized aggregates in two series of $(PEO)_{30}MeI$ systems at the end of the MD trajectory, simulated at 65 °C. N_T is the total number of aggregates.

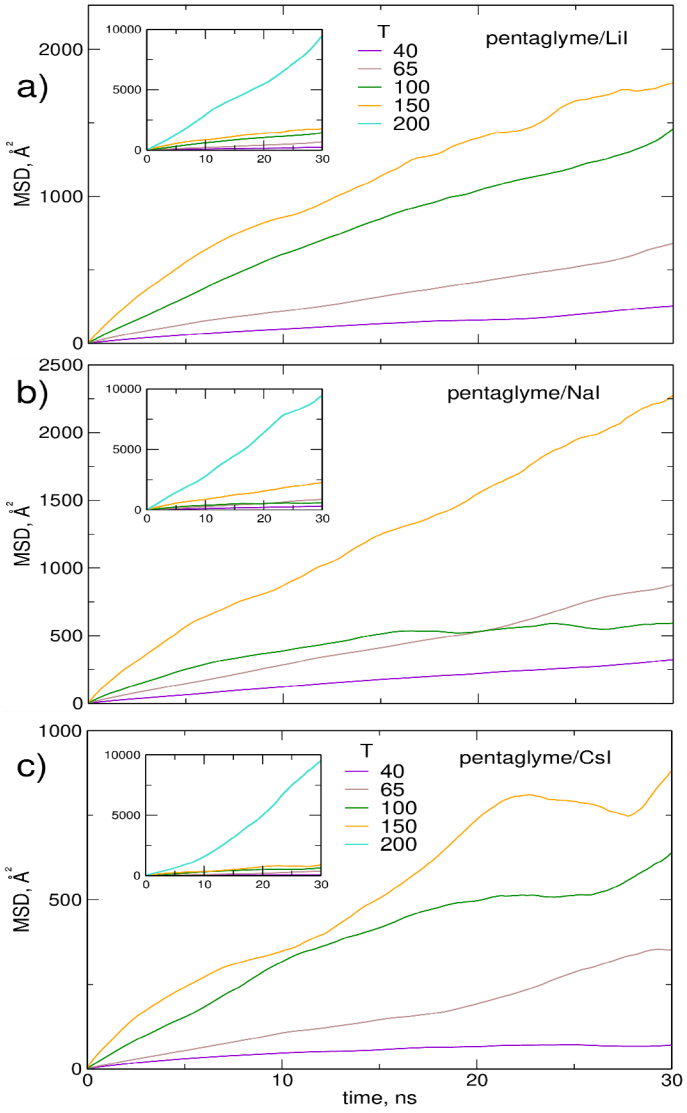

Figure S8. Averages of mean square displacement of cations and anions in pentaglyme/MeI electrolytes with Me = (a) Li, (b) Na, and (c) Cs.

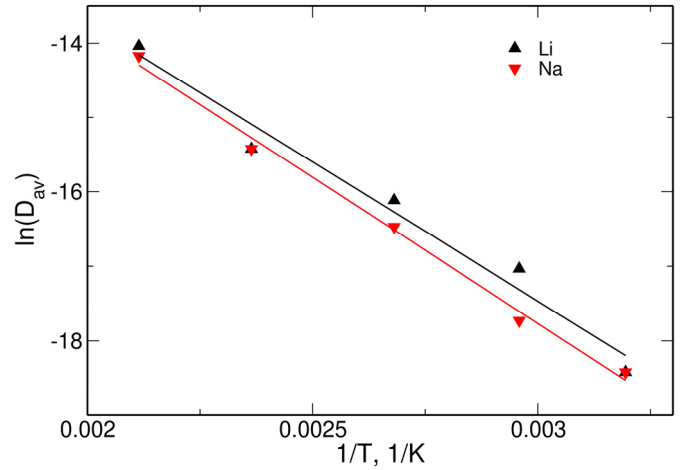

Figure S9. The dependence of ln(Dav) versus inverse of the temperature for (PEO)30LiI and (PEO)30NaI systems. Lines are linear fits to the data.

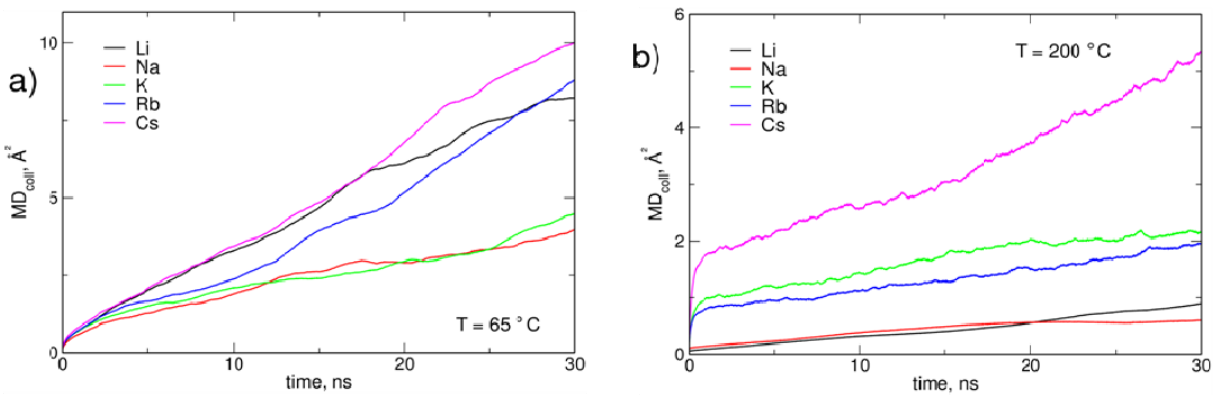

Figure S10. Collective mean displacements of ions in $(PEO)_{30}$MeI electrolytes at (a) 65 ºC and (b) 200 ºC.

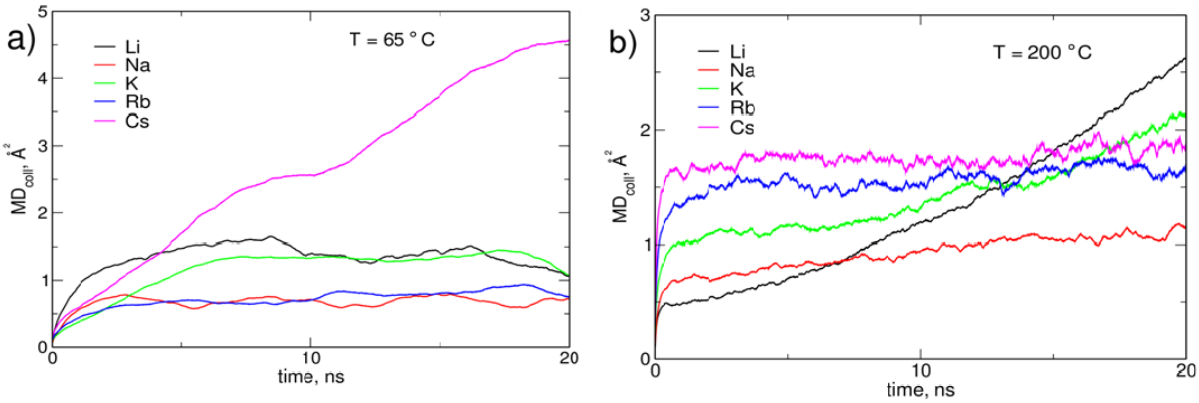

Figure S11. Collective mean displacements of ions in pentaglyme/MeI electrolytes at (a) 65 ºC and (b) 200 ºC.